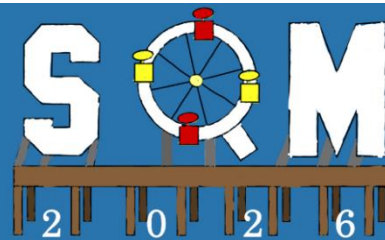


The 22nd International Conference on
Strangeness in Quark Matter
22-27 March, 2026, Los Angeles, CA



STAR Highlight II: Study of Small Systems and the Search for New, Exotic Physics

Jiangyong Jia for the STAR collaboration

Stony Brook University and BNL



STAR collaboration

25 years of RHIC: what's new from STAR

~30 energies in Au+Au
12 species combinations

- Enable a rich physics program
- Will keep us busy for 10+ years

■ Exotic searches and UPC physics

- Unstable nuclei (${}^4\text{Li}$, ${}^5\text{Li}$), muonic atoms ($\text{K}-\mu$), coherent photoproduction

■ The onset of QGP signature in O+O collisions

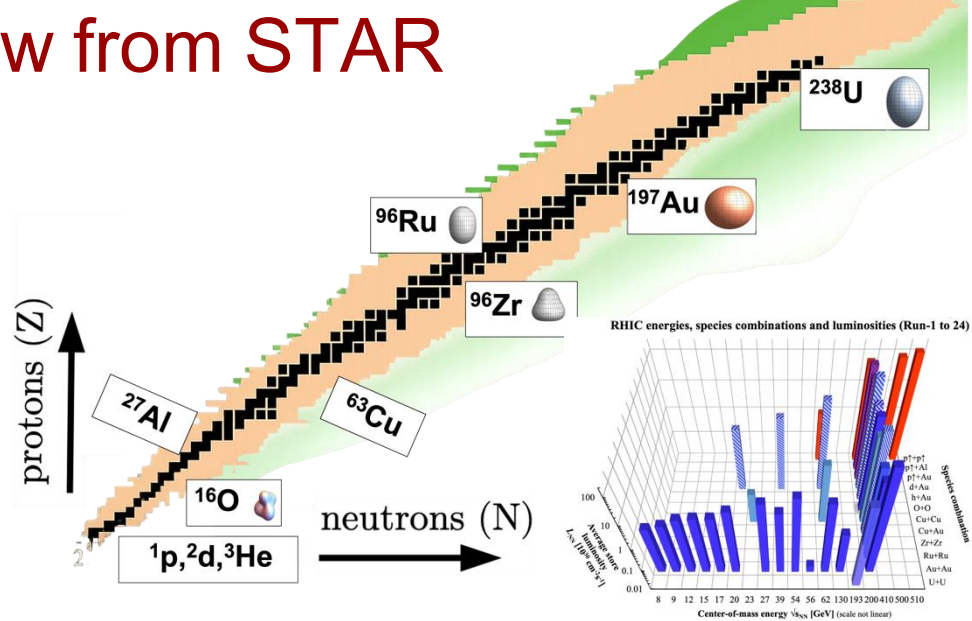
- Jet quenching, quarkonium, thermal radiation, anisotropic flow.

■ New measurements of radial flow and its fluctuations

- c_s^2 extraction, mean- p_T fluctuations, sensitivity to bulk viscosity

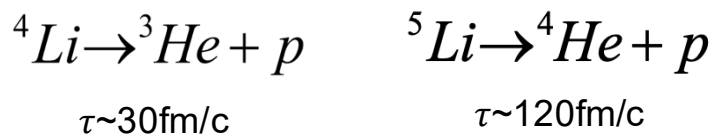
■ Polarization and spin correlations

- ϕ spin density matrix, s - $s^{\bar{}}$ correlations

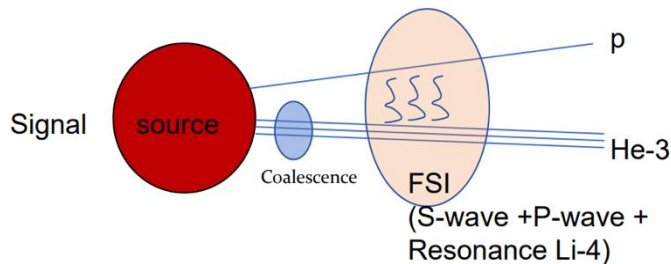


Exotic searches and UPC physics

Unstable ${}^4\text{Li}$ and ${}^5\text{Li}$ in dense medium at 3 GeV Talk: Junlin Wu (Tue)

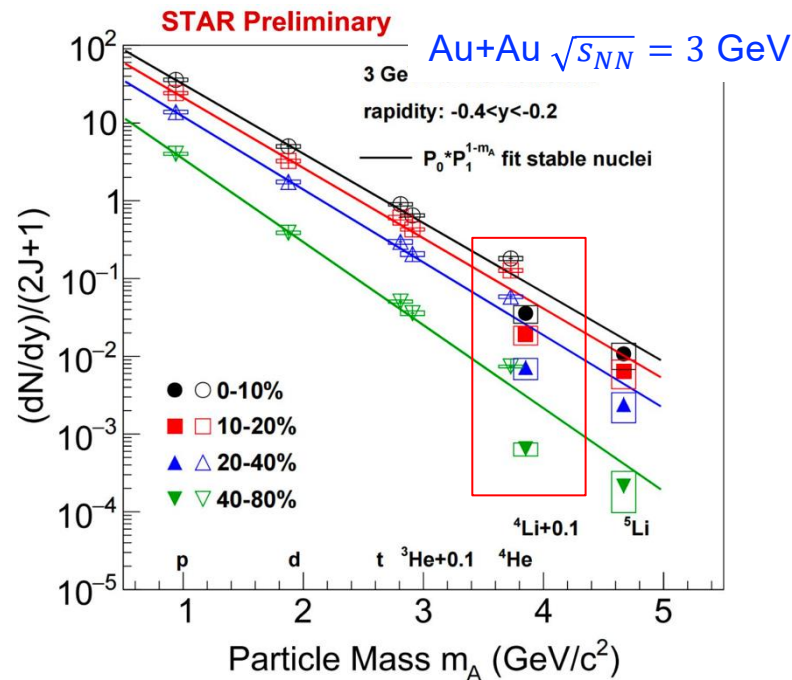


The coalescence into transient resonances is coupled with the scattering process



Novel method developed to correct for FSI interactions

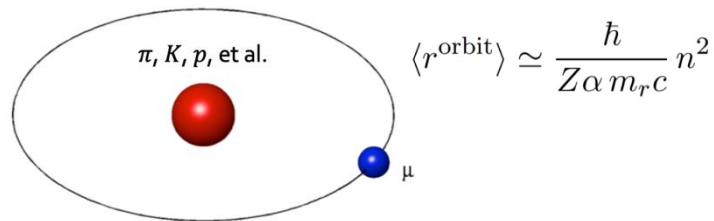
Yield of ${}^4\text{Li}$ is significantly lower than that of ${}^4\text{He}$. i.e. deviation from coalescence baseline



Unstable light nuclei provide a unique way to test light-ion production mechanism

Evidence of muonic atom: K- μ

A muon-hadron bound state



Joseph I. Kapusta and Agnes Mocsy, Phys. Rev. C 59, 2937-2940 (1999);
Xiaofeng Wang et al. Phys. Lett. B 861,13924,2(2025)

- Yield is enhanced in HIC via EM coalescence.

$$\frac{dN_a}{dyd^2p_{T,a}} = \frac{4\pi}{3} (2\alpha\hbar c/r_0)^{3/2} m_{\text{red}}^{1/2} \frac{dN_h}{dyd^2p_{T,h}} \frac{dN_l}{dyd^2p_{T,l}}$$

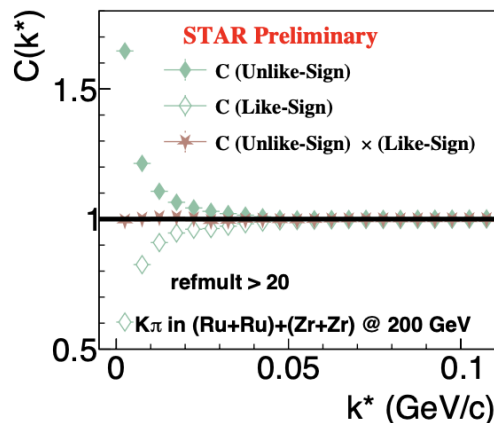
- Sensitive to yield of soft μ from QGP radiation ($p_T \sim 0.2$ GeV/c)
- Dissociation in material in flight \rightarrow shift in M_{inv}

$$\delta m \equiv M_{\text{inv}} - m_{\mu} - m_{\text{hadron}}$$

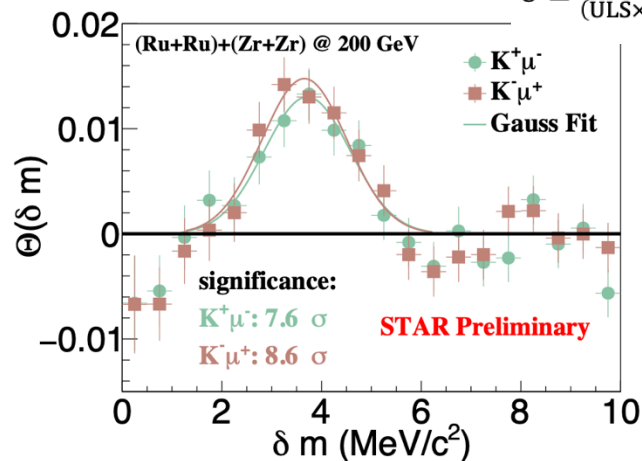
- Measure muonic atoms via K- μ momentum correlations

Suppress coulomb correlation via ULS x LS

$$\Theta \equiv \frac{(\text{ULS} \times \text{LS})_{\text{same event}}}{(\text{ULS} \times \text{LS})_{\text{mixed event}}} - 1$$

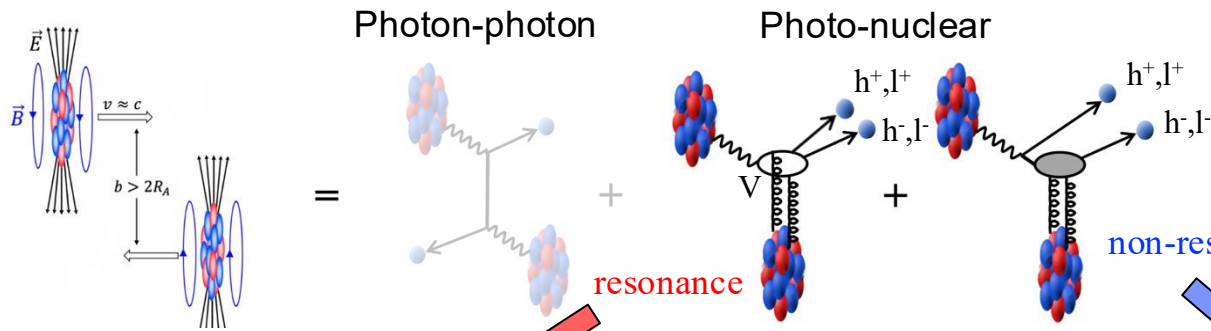


Ru+Ru, Zr+Zr
 $\sqrt{s_{NN}} = 200$ GeV



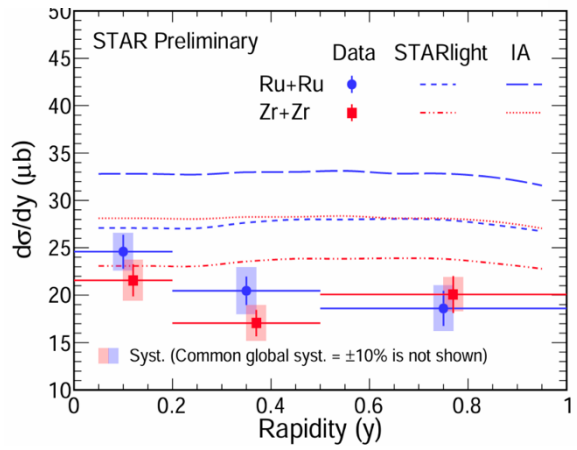
Significant signal observed, work ongoing to understand acceptance corrections

J/ψ and K⁺K⁻ photoproduction in UPC

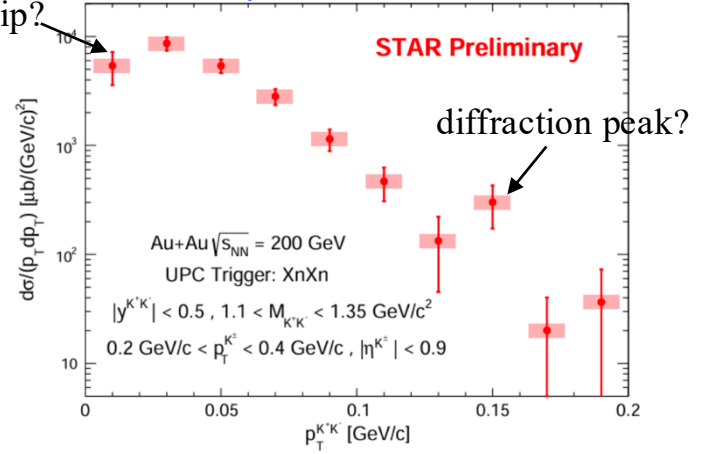


$\gamma^* + A \rightarrow J/\psi + A^* \rightarrow e^+e^- + A^*$

$\gamma^* + A \rightarrow K^+ + K^- + A^*$



Interference dip?



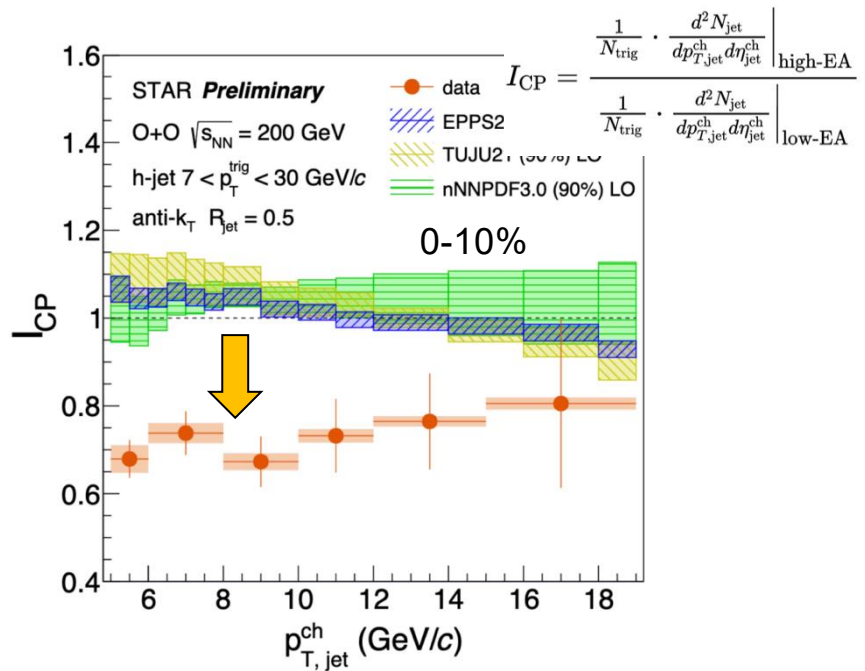
Coherent J/ψ yields suggest strong suppression compared to baseline models

Most precise measurement of coherent non-resonant K⁺K⁻ production

Search for onset of QGP signature in O+O

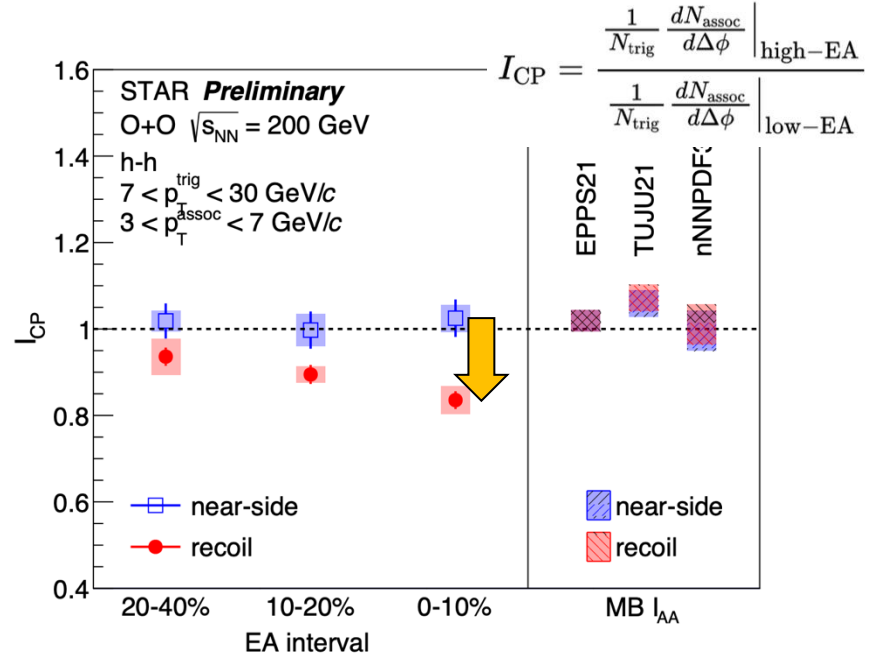
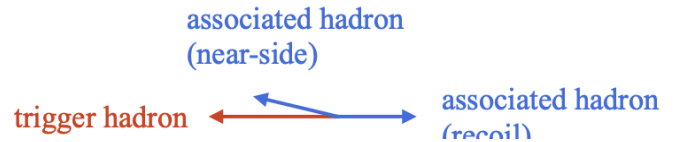
Evidence of jet quenching in O+O

hadron-jet correlations



Event activity (EA) defined in forward detectors to reduce bias

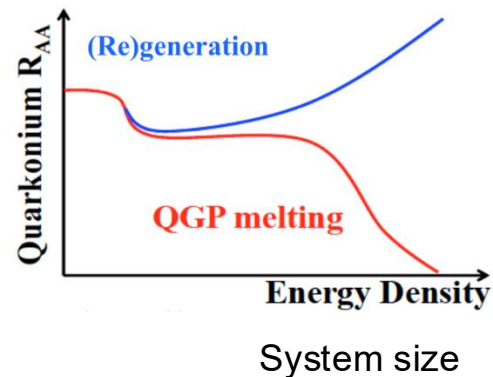
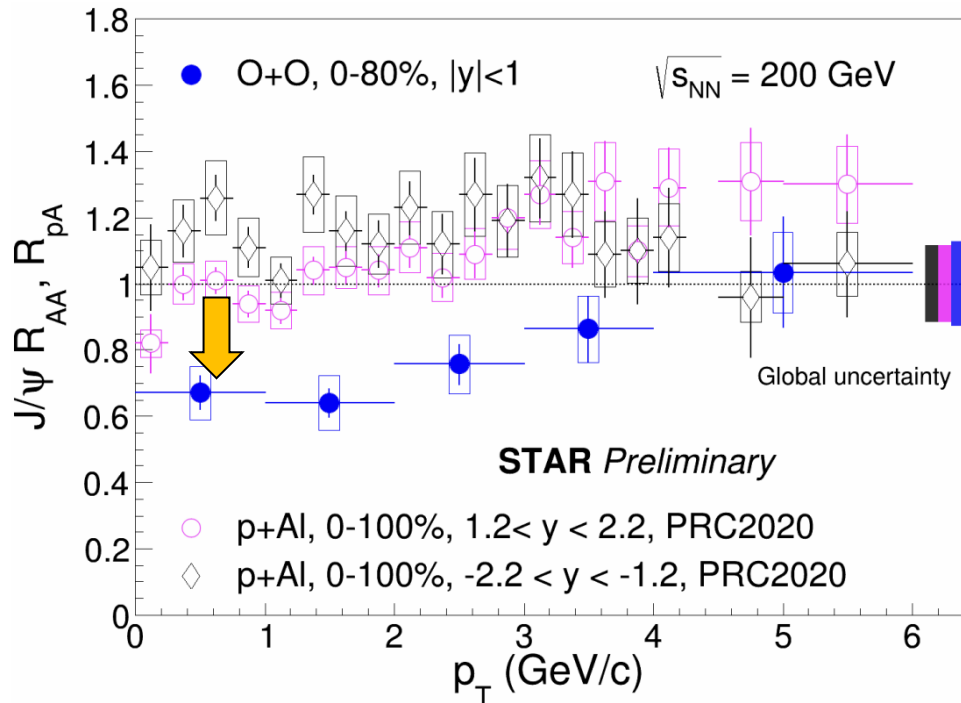
hadron-hadron correlations



J/ψ production in O+O

Sensitive to both hot QGP medium and cold nuclear matter effects.

- O+O has small CNM effects, provides an important anchor point.

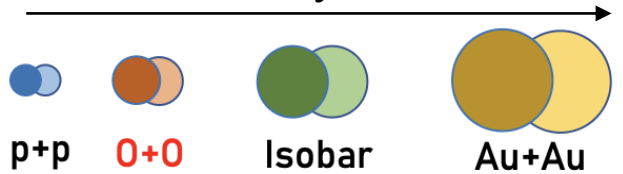


Clear suppression beyond the expected CNM effects \rightarrow hot medium effect?

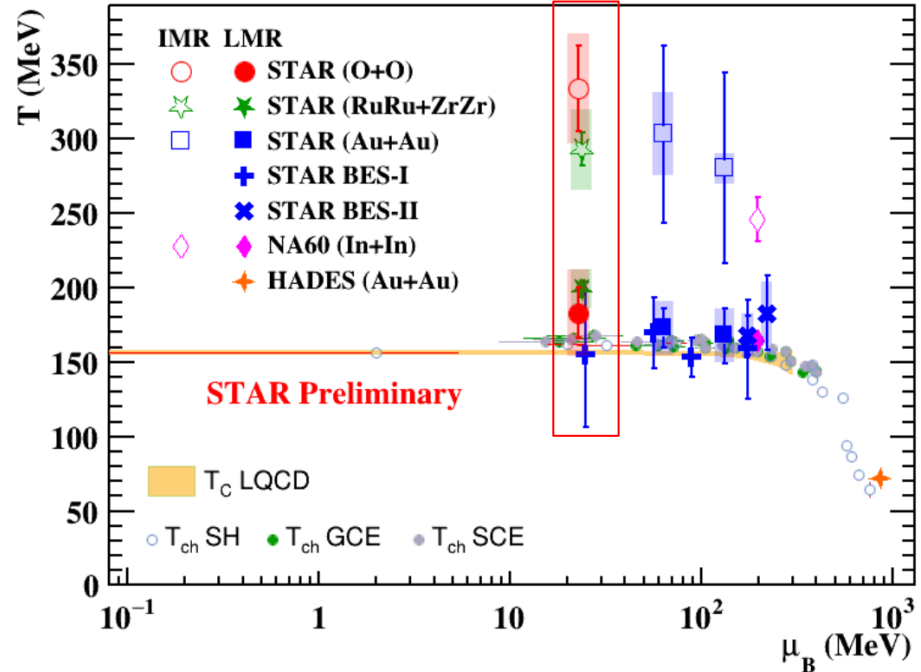
Dilepton production in O+O

Dileptons are thermometer of QGP

Increase in system size



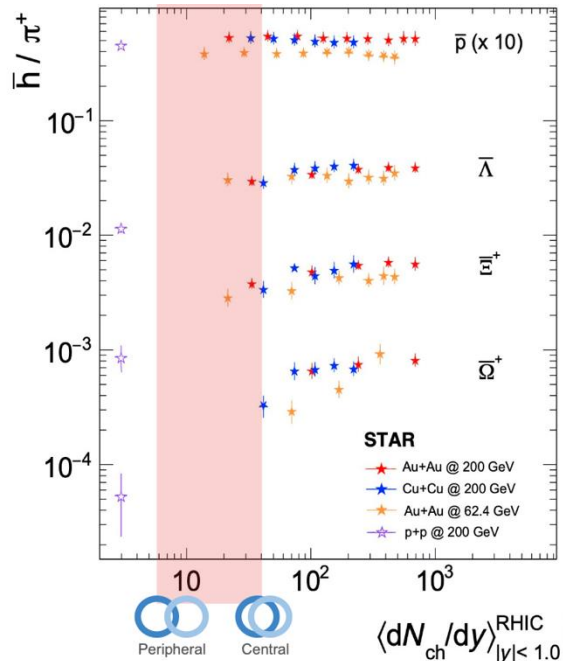
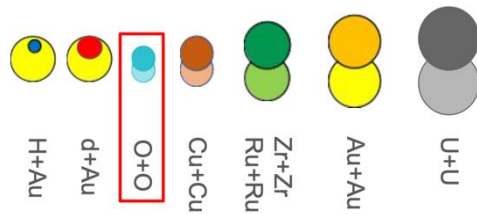
Higher density but shorter lifetime



Temperature measured in LMR (near phase transition) and IMR (QGP dominant)
 Temperature in O+O is as high as in large isobar systems

Consistent with thermal radiation from the QGP medium

Strangeness production in O+O

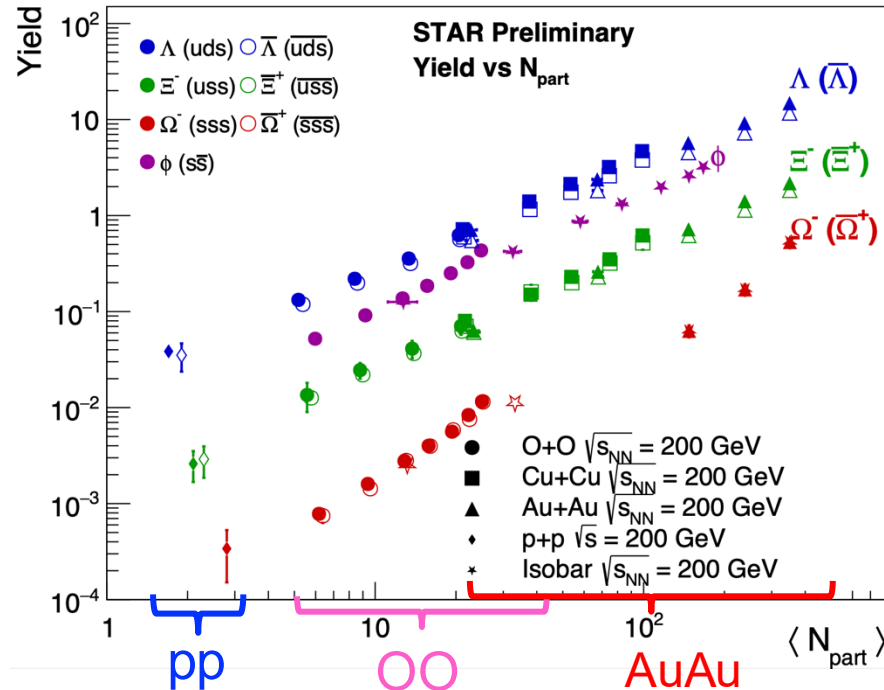


Motivation:

- strangeness/pion ratios increase with N_{ch} at RHIC, like LHC.
- but large gap at onset region, which O+O data can fill.

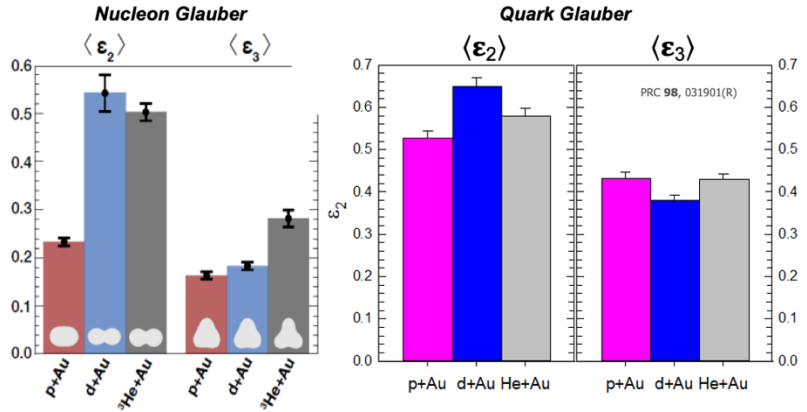
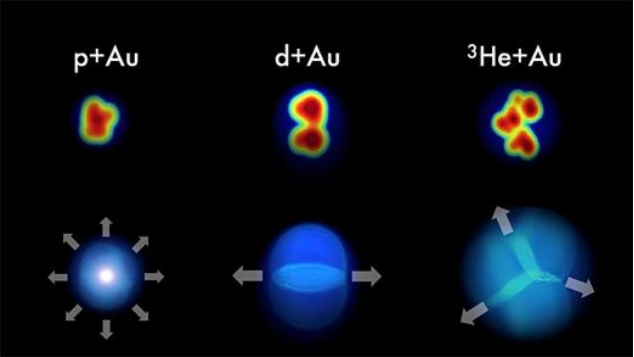
Result:

- Yields of Ω/ϕ , $\bar{\Lambda}/\Lambda$, $\bar{\Xi}^-/\Xi^+$, Ω^-/Ω^+ ... vs N_{part}
- We see smooth transition from small to large systems



Flow in small systems

Goal: Show that flow is driven by initial-state geometry though QGP response



Challenge: p/d/³He+Au ordering reflects interplay between nucleonic and subnucleonic fluctuations

$$\epsilon_2^{3\text{HeAu}} \approx \epsilon_2^{d\text{Au}} > \epsilon_2^{p\text{Au}}$$

$$\epsilon_3^{3\text{HeAu}} \approx \epsilon_3^{d\text{Au}} > \epsilon_3^{p\text{Au}}$$

$$\epsilon_2^{3\text{HeAu}} \approx \epsilon_2^{d\text{Au}} \gtrsim \epsilon_2^{p\text{Au}}$$

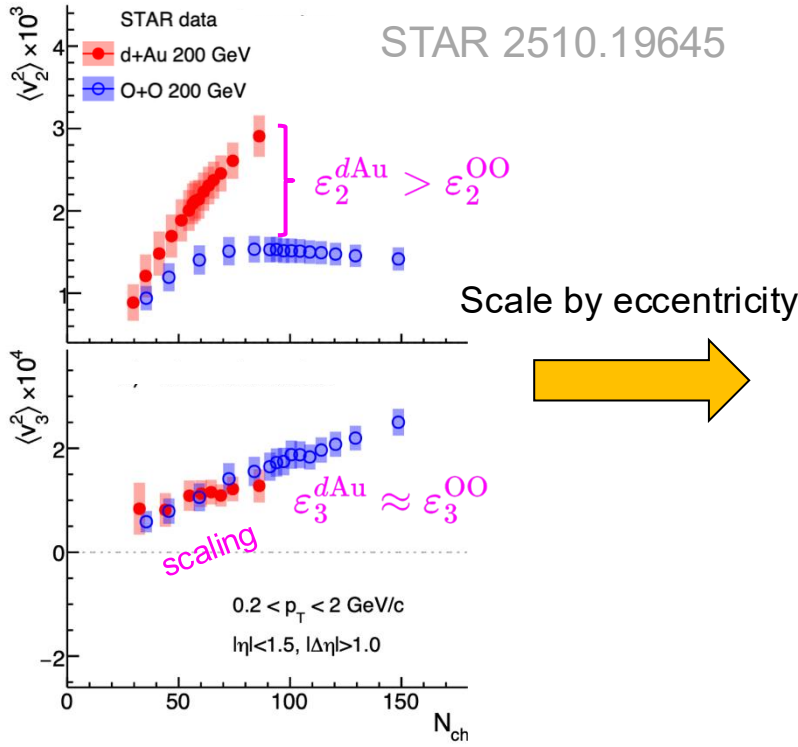
$$\epsilon_3^{3\text{HeAu}} \approx \epsilon_3^{d\text{Au}} \approx \epsilon_3^{p\text{Au}}$$

Constrain subnucleonic fluctuations by comparing d+Au with ¹⁶O+¹⁶O

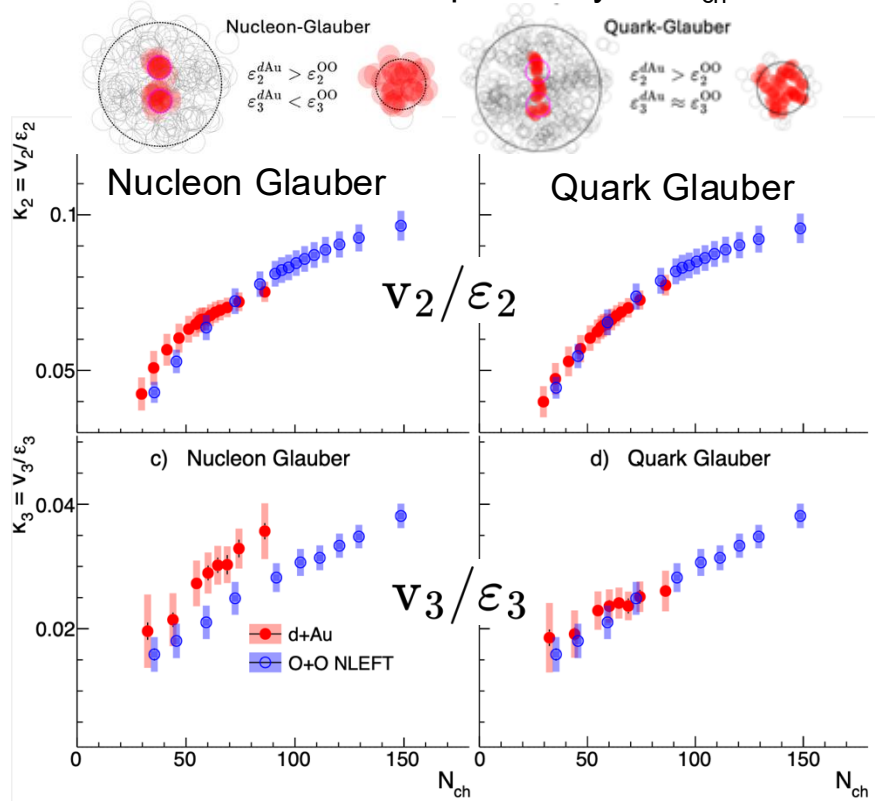
NB: Nucleon configurations of deuteron or ¹⁶O are well constrained in ab initio models.

Compare d+Au and O+O flow data

Characteristic ordering driven by geometry is observed

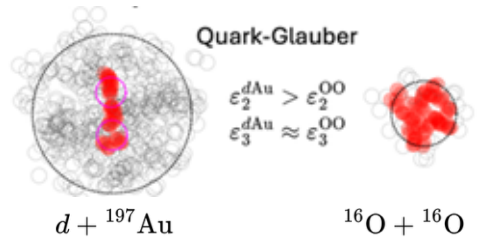


$k_n = v_n / \epsilon_n$ reflecting hydrodynamic response, should depend only on N_{ch}



Better scaling achieved when considering substructure fluctuations

Compare d+Au and O+O elliptic flow fluctuations



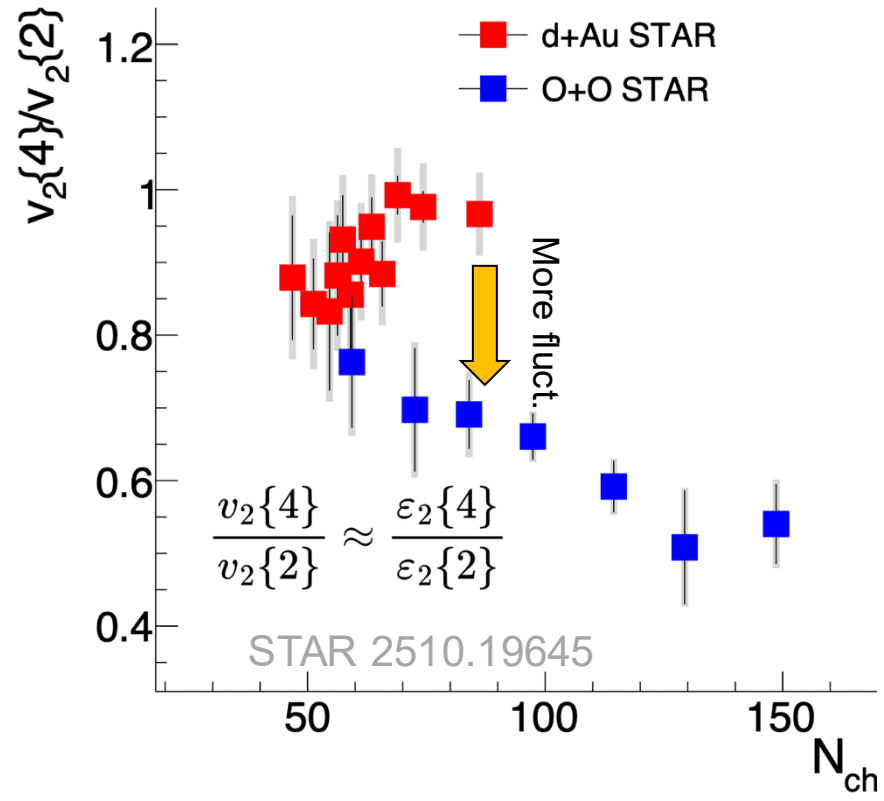
Small fluctuations in dAu

$$\frac{v_2^{dAu}\{4\}}{v_2^{dAu}\{2\}} \approx \frac{\epsilon_2^{dAu}\{4\}}{\epsilon_2^{dAu}\{2\}} \approx 0.9$$

Large fluctuations in OO

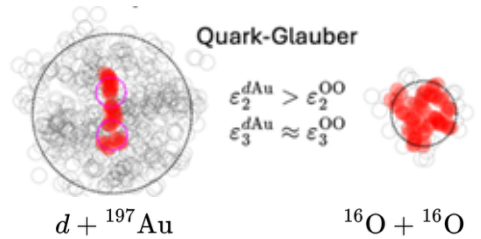
$$\frac{v_2^{OO}\{4\}}{v_2^{OO}\{2\}} \approx \frac{\epsilon_2^{OO}\{4\}}{\epsilon_2^{OO}\{2\}} \sim 0.6$$

Compare to ATLAS data
(re-match to STAR centrality)



Fluctuations universal with $\sqrt{s_{NN}}$ despite x10 (x3) increase in energy (multiplicity)

Compare d+Au and O+O elliptic flow fluctuations



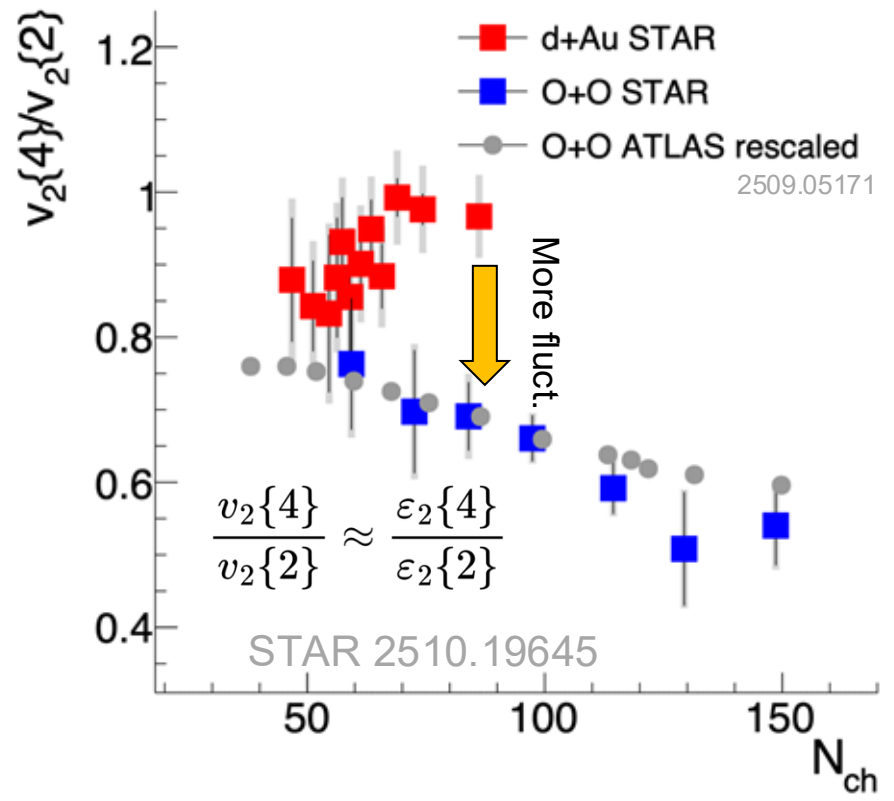
Small fluctuations in dAu

$$\frac{v_2^{dAu}\{4\}}{v_2^{dAu}\{2\}} \approx \frac{\epsilon_2^{dAu}\{4\}}{\epsilon_2^{dAu}\{2\}} \approx 0.9$$

Large fluctuations in OO

$$\frac{v_2^{OO}\{4\}}{v_2^{OO}\{2\}} \approx \frac{\epsilon_2^{OO}\{4\}}{\epsilon_2^{OO}\{2\}} \sim 0.6$$

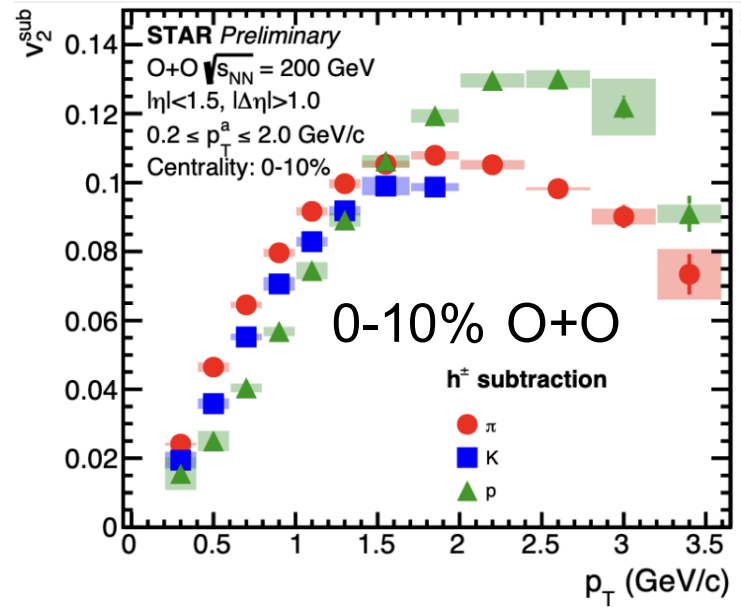
Compare to ATLAS data
(re-match to STAR centrality)



Fluctuations universal with $\sqrt{s_{NN}}$ despite x10 (x3) increase in energy (multiplicity)

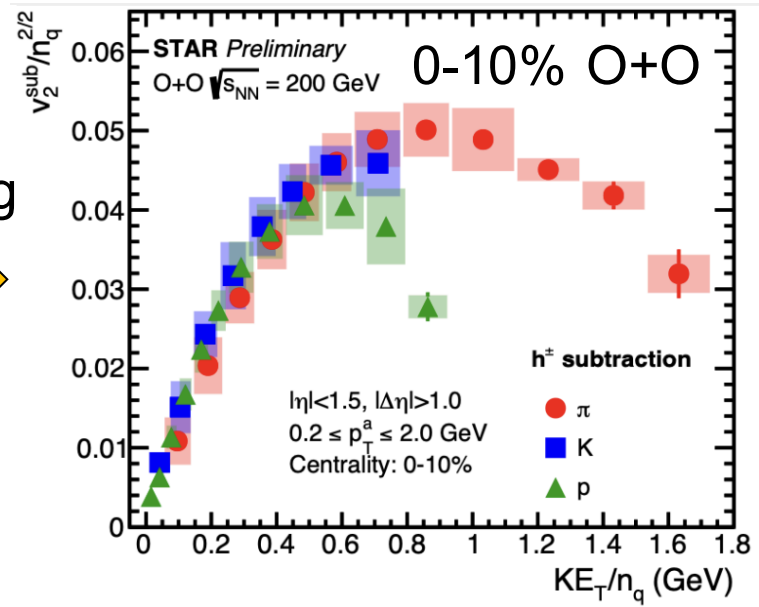
$\pi/K/p$ elliptic flow in central O+O collisions

v_2 for $\pi/K/p$ (non-flow subtracted)



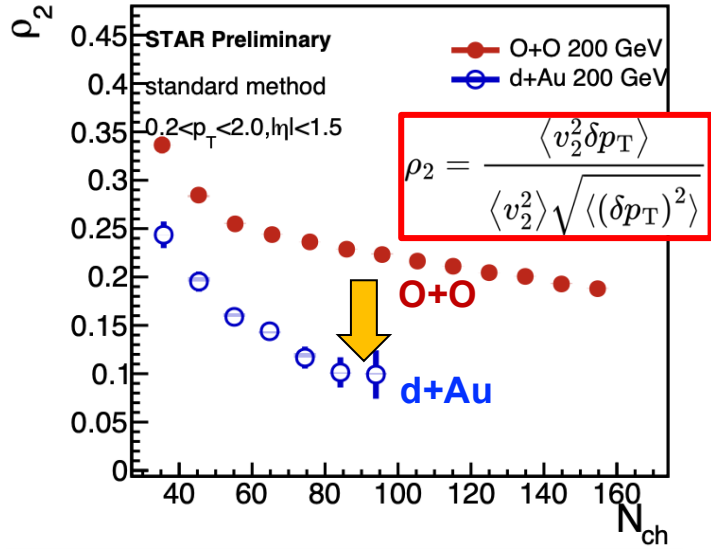
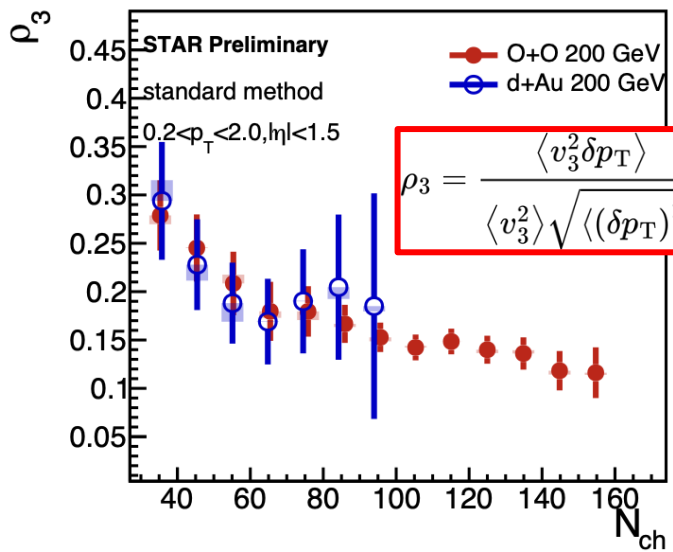
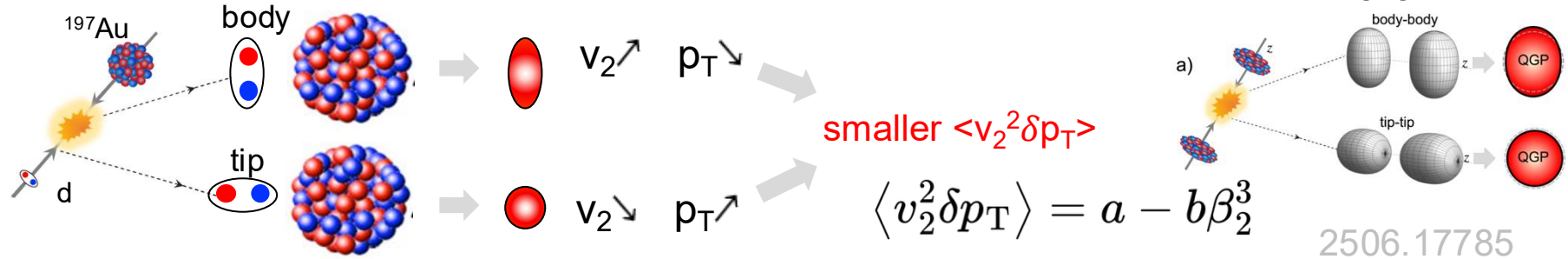
NCQ-scaling

Scaled by number of quarks



- Significant hierarchy for identified particles expected for v_2 .
- Follow NCQ-scaling at low p_T , but deviation at higher p_T .

Impact of prolate shape of deuteron

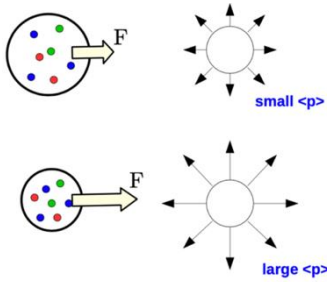


Behavior of $\langle v_2^2 \delta p_T \rangle$ consistent with QGP response to the prolate shape of deuteron 17

Radial flow and its fluctuations

Radial flow observables

Large event-by-event fluctuations



$$p_T \approx p_T^{th} + m \langle v_T \rangle$$

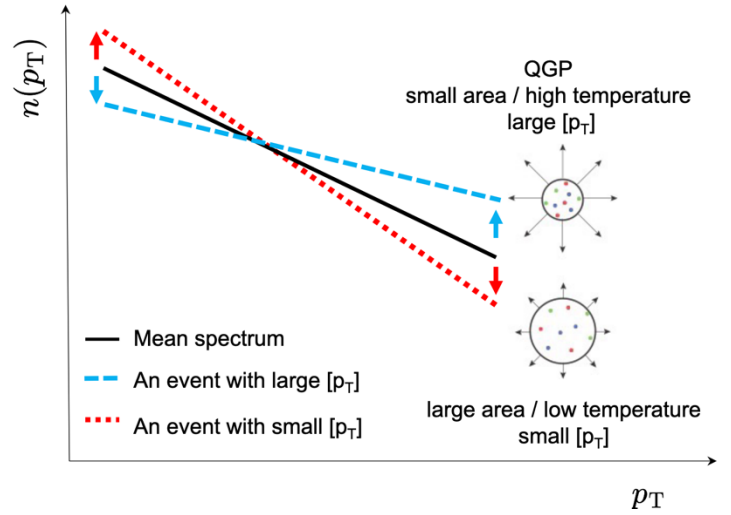
Response to size fluctuations

$$\delta p_T / \langle [p_T] \rangle \approx -\delta R / \langle R \rangle$$

Integral: $\langle [p_T] \rangle, v_{0,int} \equiv \frac{\sqrt{\langle (\delta [p_T])^2 \rangle}}{\langle [p_T] \rangle}$

Fluctuation of local yield $\delta n(p_T)$ and $\delta [p_T]$ are correlated \rightarrow measure $\langle \delta n(p_T) \delta [p_T] \rangle$.

differential: $v_0(p_T) v_{0,int} = \frac{\langle \delta n(p_T) \delta [p_T] \rangle}{\langle n(p_T) \rangle \langle [p_T] \rangle}$



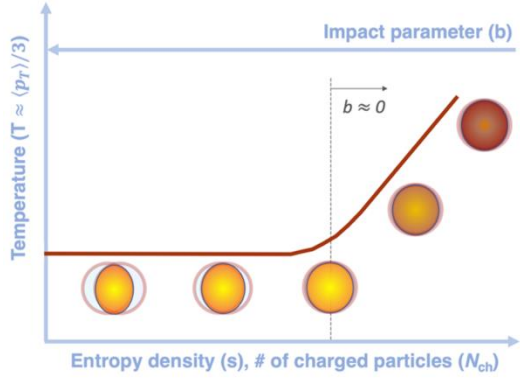
Extraction of speed of sound from $\langle p_T \rangle$

$\langle p_T \rangle$ increase with N_{ch} in UCC are related to the Temperature fluctuations $\rightarrow c_s^2$

$$c_s^2 = \frac{dP}{d\varepsilon} \approx \frac{d(\ln \langle p_T \rangle)}{d(\ln N_{ch})} \quad \text{or} \quad \frac{\Delta_{p_T}}{\langle p_T \rangle} = c_s^2 \frac{\Delta_N + \delta}{N}$$

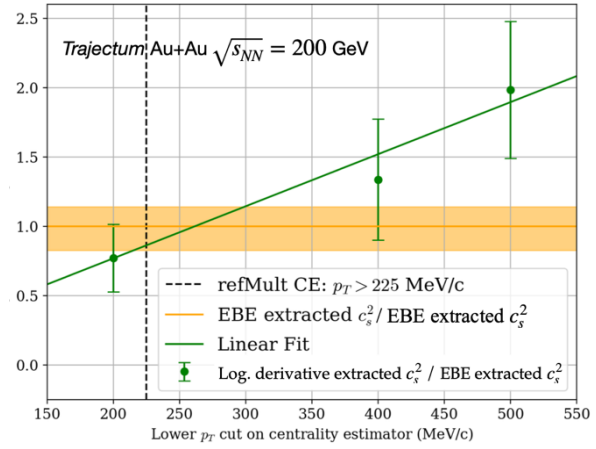
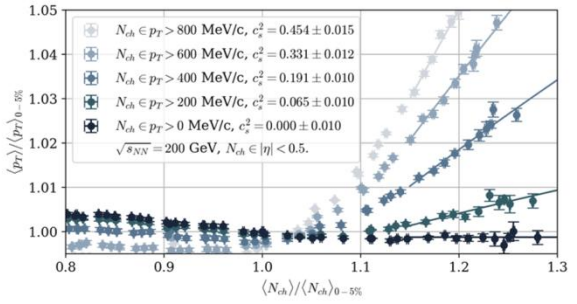
1908.09728 2501.02777

e-by-e model fluctuations



- Enforcing the following consistency in Trajectum model:
- c_s^2 obtained via (2) by imposing constraint $\{\delta^3\}=0$
 - c_s^2 obtained via (1) for N_{ch} defined with $p_T > p_{Tmin}$
 - vary p_{Tmin} for N_{ch} until (1) agree with (2)

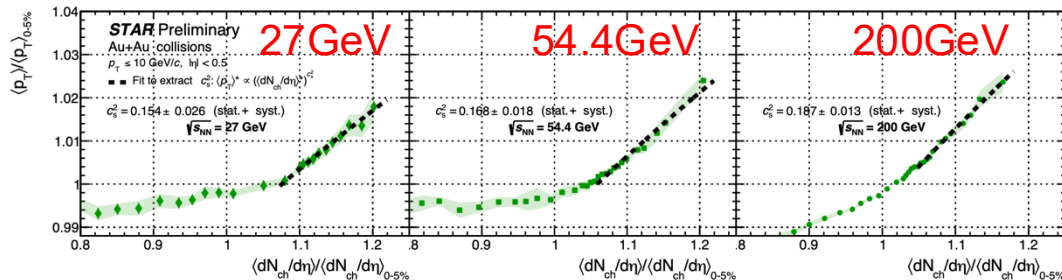
Relation (1) is broken by acceptance effects in defining centrality estimator N_{ch} .



suggests $p_{T,min} = 0.225$ GeV for centrality estimator

Extraction of speed of sound from $\langle p_T \rangle$

Extract c_s^2 in three energies:

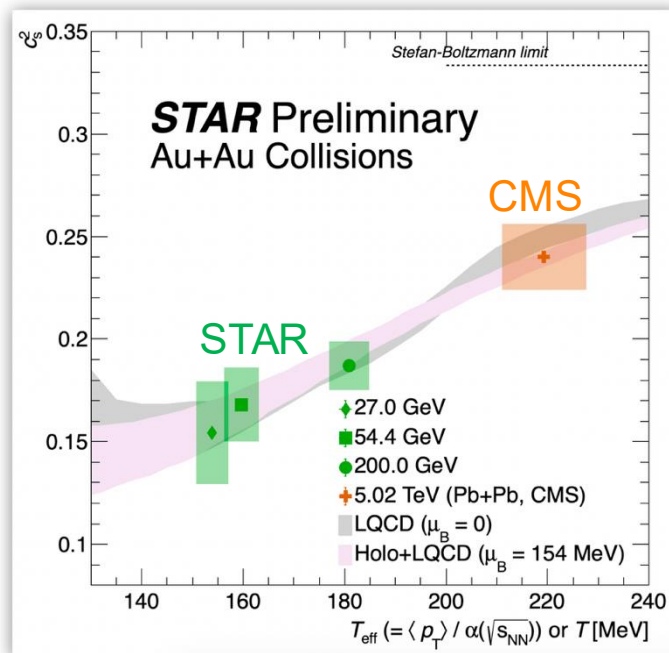


To estimate T_{eff} :

- First estimate $\langle p_T \rangle$ by extrapolating to zero p_T .
- $T_{\text{eff}} = \alpha \langle p_T \rangle / 3$, α estimated from hydro model, close to 1

2403.06052

First extraction of temperature dependence of c_s .
Result consistent with LQCD!

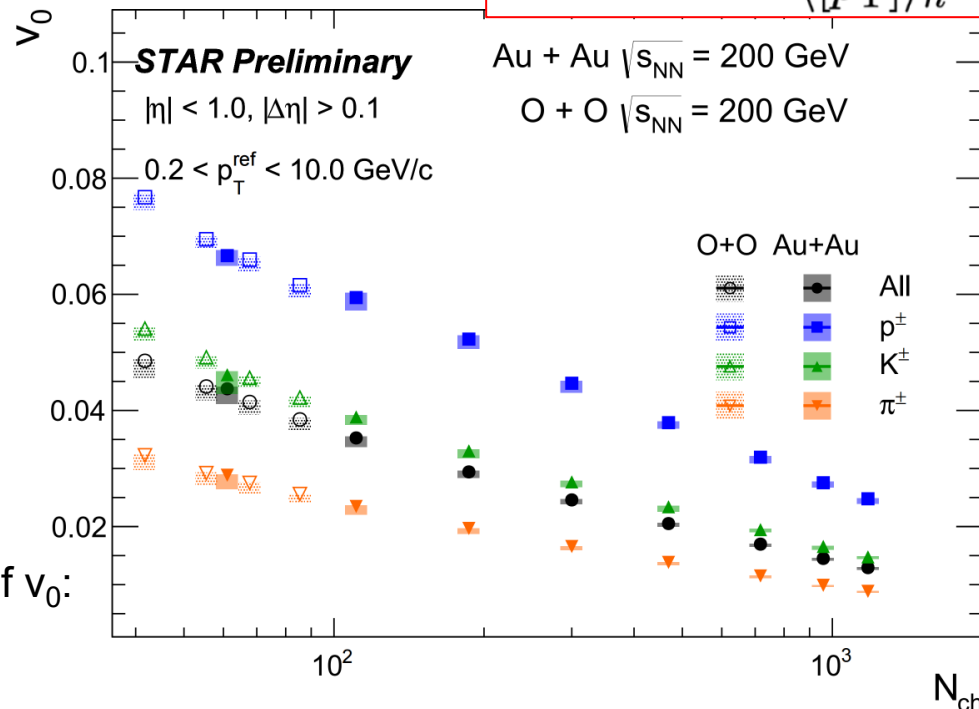


v_0 : Integral p_T fluctuation at 200 GeV

- Measured for charged hadrons, protons, kaons and pions in OO to AuAu.
- larger fluctuation signals for heavier particles.
- v_0 follows an approximate power scaling $v_0 \sim 1/\sqrt{N_{ch}}$.

Expected for independent source model

$$v_{0,PID} = \frac{\langle \delta[p_T]_{PID} \delta[p_T]_h \rangle}{\langle [p_T] \rangle_h}$$

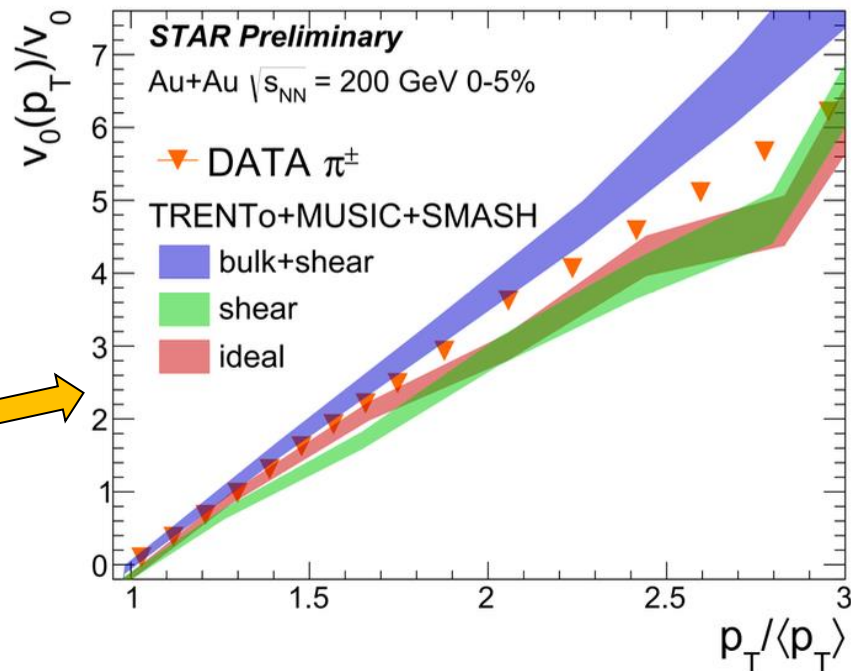
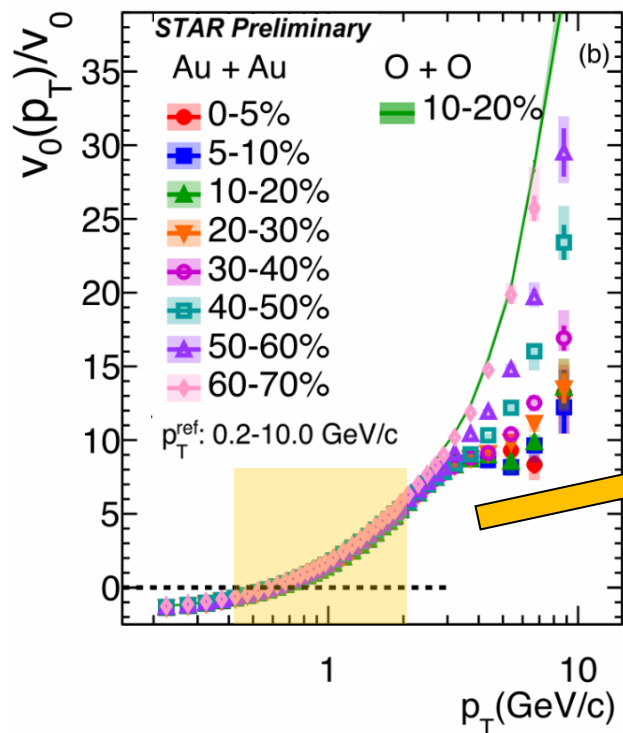


Also see Rutik's talk for $\sqrt{s_{NN}}$ dependence of v_0 :

Talk: Rutik Manikandhan (Tue)

$v_0(p_T)$: p_T -differential fluctuations at 200 GeV

$v_0(p_T)$ and v_0 are driven by size fluctuations, use $v_0(p_T)/v_0$ to take out overall fluctuations



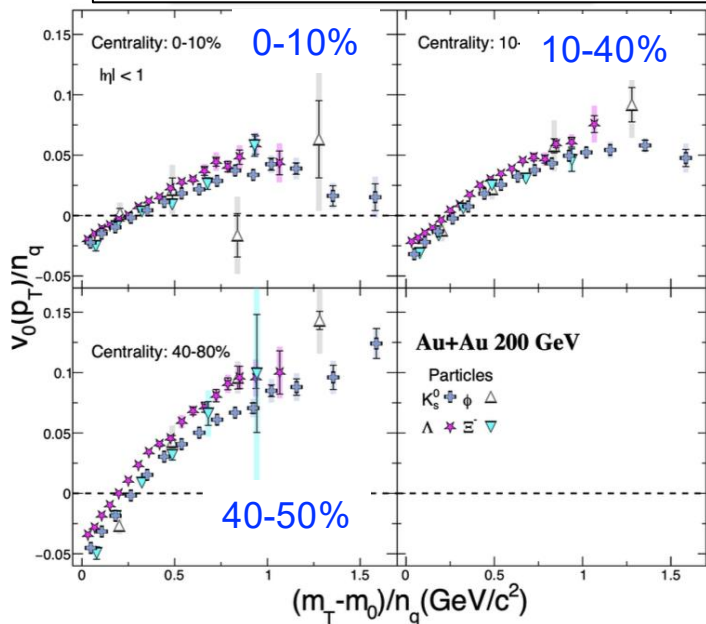
Universal shape scaling across centrality and systems, except at high p_T

Intermediate p_T region shows clear sensitivity to bulk viscosity.

$v_0(p_T)$: strange hadron and its $\sqrt{s_{NN}}$ dep.

PID (strange meson and baryons) dependence allows a detailed test of NCQ scaling

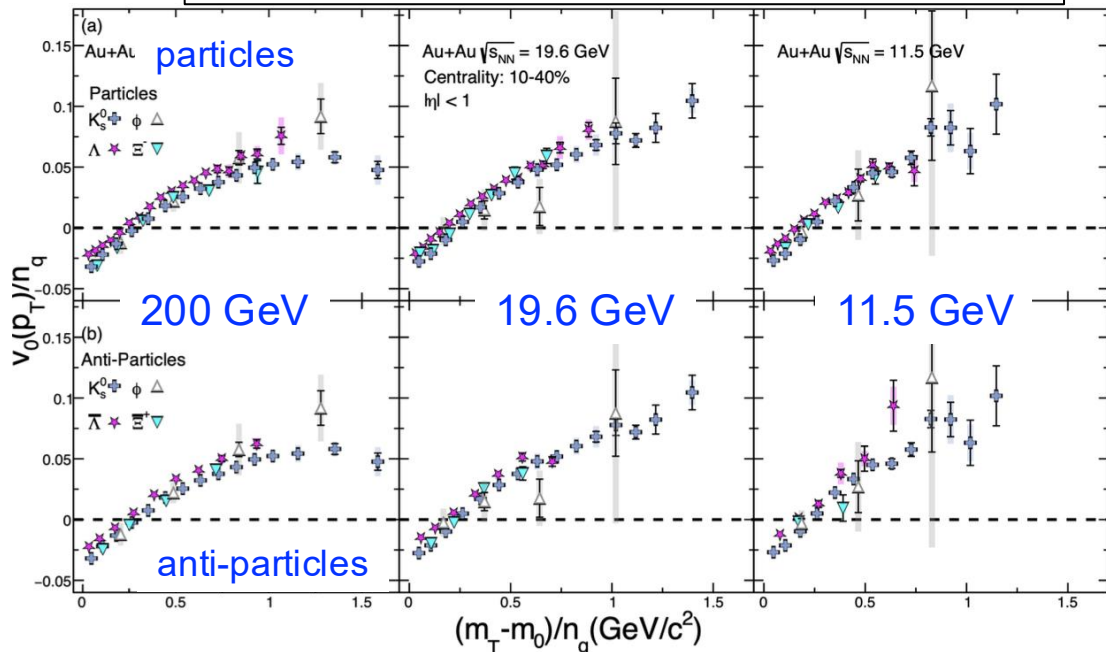
Centrality dependence at 200 GeV



deviation in more peripheral collisions

Look forward to theory predictions!

Energy dependence in 10-40% centrality collisions



approximately hold in broad $\sqrt{s_{NN}}$ range

signal also change weakly with $\sqrt{s_{NN}}$

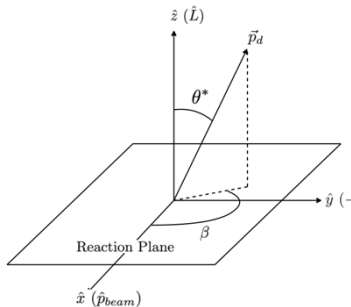
Polarization and spin correlations

ϕ -meson spin alignment via $\phi(ss\bar{)} \rightarrow K^+K^-$

spin-density matrix

$$\rho = \begin{pmatrix} \rho_{-1-1} & \rho_{-1,0} & \rho_{-11} \\ \rho_{0-1} & \rho_{00} & \rho_{01} \\ \rho_{1-1} & \rho_{10} & \rho_{11} \end{pmatrix}$$

coordinate choice

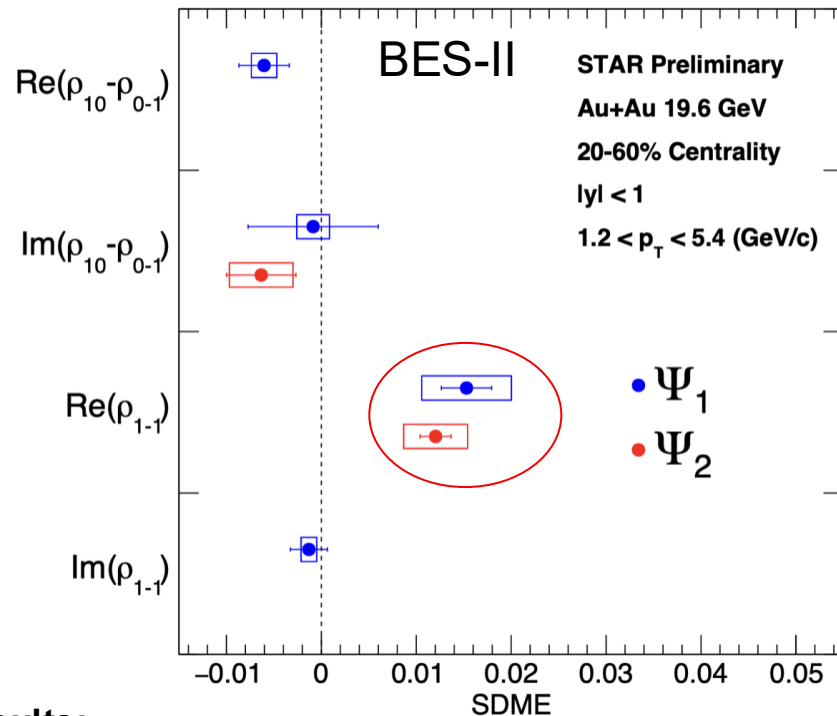


general 2D distribution of daughter K

$$\frac{d^2N}{d \cos \theta^* d\beta} = \frac{3}{8\pi} \left[(1 - \rho_{00}) + (3\rho_{00} - 1) \cos^2 \theta^* \right. \\ \left. - \sqrt{2} \operatorname{Re}(\rho_{10} - \rho_{0-1}) \sin 2\theta^* \cos \beta \right. \\ \left. + \sqrt{2} \operatorname{Im}(\rho_{10} - \rho_{0-1}) \sin 2\theta^* \sin \beta \right. \\ \left. - 2 \operatorname{Re}(\rho_{1-1}) \sin^2 \theta^* \cos 2\beta \right. \\ \left. + 2 \operatorname{Im}(\rho_{1-1}) \sin^2 \theta^* \sin 2\beta \right],$$

Motivation:

- Previous measurements assume off-diagonal terms are zero and only measure θ^* dep. $\rightarrow \rho_{00}$.
- Extend the measurement to both θ^* and β dependence to access the off-diagonal terms.
- ϕ has contribution from both s - $s\bar{}$ global polarization and spin correlations.

 $\rho_{00}^{-1/3} \sim 0.02$ at 19.6 GeV BES-I from Nature 614 244,2023**Results:**

- First measurement in Au+Au with full 2D correction
- First evidence of non-zero off-diagonal term ρ_{1-1} !
- Signal is large, suggests non-zero s - $s\bar{}$ spin correlations.

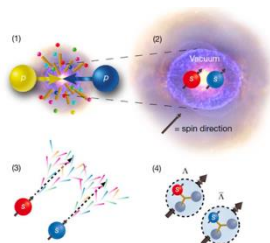
s - \bar{s} spin correlations

$$\langle P_q P_{\bar{q}} \rangle \neq \langle P_q \rangle \langle P_{\bar{q}} \rangle$$

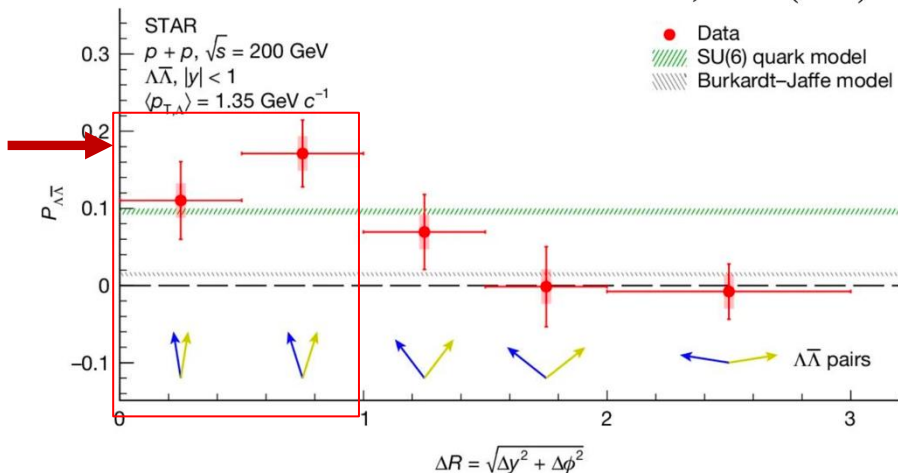
Such spin correlations was in fact observed in p+p collisions!

Measurement of $\Lambda\bar{\Lambda}$ correlation suggest maximum $s\bar{s}$ spin correlations:

Properties of QCD vacuum: $J^{PC} = 0^{++}$



STAR Collaboration. Nature 650, 65–71 (2026).



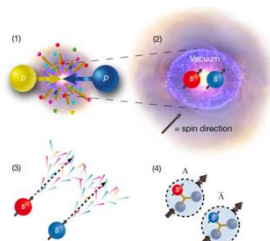
s - \bar{s} spin correlations

$$\langle P_q P_{\bar{q}} \rangle \neq \langle P_q \rangle \langle P_{\bar{q}} \rangle$$

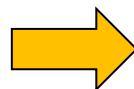
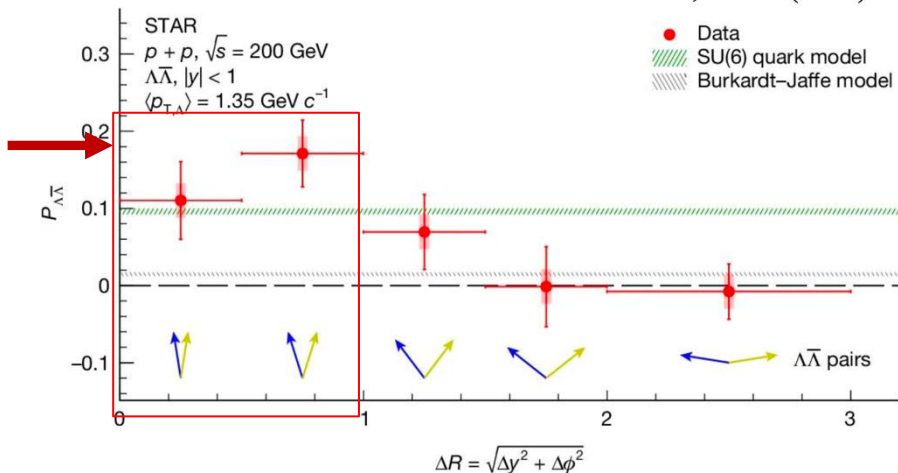
Such spin correlations was in fact observed in p+p collisions!

Measurement of $\Lambda\bar{\Lambda}$ correlation suggest maximum $s\bar{s}$ spin correlations:

Properties of QCD vacuum: $J^{PC} = 0^{++}$

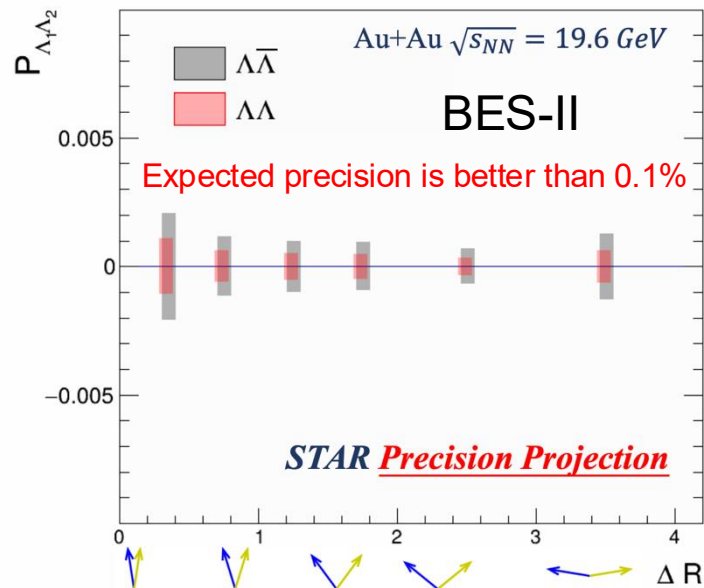


STAR Collaboration. Nature 650, 65–71 (2026).



What happens to QCD vacuum at finite temperature?

Measurement of $\Lambda\bar{\Lambda}$ correlation is ongoing.



Summary

STAR's rich datasets, 40+ species combinations or energies, are a gold mine for a diverse physics program

- First observations of ${}^4\text{Li}$, ${}^5\text{Li}$, muonic atom, precision photonuclear J/ψ , K^+K^- measurement.
- Multiple independent probes provide strong evidence for QGP formation in central O+O.
- New utilities of radial flow to probe speed of sound and bulk viscosity.
- First measurement of off-diagonal spin density-matrix and spin-spin correlations for s - \bar{s}

More discoveries in the decades to come.

List of STAR Presentations

| TITLES | PRESENTER | DAY/SESSION (with LINK) |
|---|-------------------|-----------------------------|
| Parallel Talks: | | |
| 1. Strange hadron production in different collision systems at sNN = 200 GeV at STAR Beam Energy Scan-II at STAR | Iris Ponce | Tue, P1 |
| 2. Exploring Strangeness Production across Beam Energies in Au+Au Collisions at STAR | Weiguang Yuan | Tue, P1 |
| 3. Measurement of Charge Symmetry Breaking in A = 4 hypemuclei in sNN = GeV Au+Au collisions at RHIC | Tianhao Shao | Tue, P1 |
| 4. Production of Unstable Light Nuclei in Au+Au Collisions at sNN = GeV with the STAR Detector | Chenlu Hu | Tue, P1 |
| 5. Light hadron production measurements with Au+Au Collisions from sNN = 3.2 -4.5 GeV with STAR | Mathias Labonte | Tue, P11 |
| 6. Extracting the Speed of Sound from Mean Transverse Momentum Measurements in Au+Au Collisions from RHIC-BESII | Caleb Broodo | Tue, P11 |
| 7. Radial Flow of Strange and Multi-strange Hadrons in Heavy-Ion Collisions at RHIC-STAR | Yuli Kong | Tue, P11 |
| 8. Collision Energy and System Size Dependent Radial Flow Fluctuations at RHIC | Zaining Wang | Tue, P11 |
| 9. Measurement of thermal dielectron production in O+O collisions at sNN = 200 GeV with the STAR experiment | Zihan Liu | Tue, P111 |
| 10. Hyperon Spin Observables in Au+Au Collisions at RHIC BES-II: Global and Local Polarization, Spin Correlations | Tong Fu | Tue, P1V |
| 11. Differential measurements of phi-meson global spin alignment and off-diagonal spin density matrix elements in Au+Au | Zhenyu Ye | Tue, P1V |
| 12. Measurements of Local Polarization of Hyperons with Event Shape Engineering in Au+Au collisions at RHIC-STAR | Taiki Kondo | Tue, P1V |
| 13. Non-Monotonicity of pT Correlations in Au + Au Collisions at RHIC | Rutik Manikandhan | Tue, P1V |
| 14. Observation of Strong Directed Flow for phi meson in High Baryon Density Region at RHIC | Guangyu Zheng | Tue, P1V |
| 15. Third-body-corrected Two-Pion Femtoscopic Correlations in Au+Au Collisions at high baryon density | Youquan Qi | Tue, P1V |
| 16. Measurements of p-Xi Correlation Functions in Au+Au Collisions from STAR Beam Energy Scan II | Jing An | Tue, P1V1 |
| 17. p-p-Lambda Correlation in 3 GeV Au+Au Collisions with the STAR Detector | Jing Gu | Tue, P1V11 |
| 18. Observation of a Strange Muonic Atom and Its Antimatter in Heavy-Ion Collisions at STAR | Zhangbu Xu | Tue, P1V111 |
| 19. Exploring System-Size and Energy Dependence of J/Psi production with the STAR experiment | Kaifeng Shen | Wed, P11 |
| 20. Fluctuations and Correlations of Conserved Charges in Isobar Collisions at sNN = 200 GeV with STAR Detector | Hanwen Feng | Wed, P1V1 |

List of STAR Presentations

| TITLES | Posters: | PRESENTER | DAY/SESSION (with LINK) |
|---|----------|------------------|----------------------------|
| 1. Search for dark photons in π^0/η Dalitz decays with the STAR detector | | Kaifeng Shen | Wed |
| 2. Bulk Properties of the medium in Ru+Ru and Zr+Zr Collisions at $\sqrt{s_{NN}} = 200$ GeV with STAR detector | | Chun Yuen Tsang | Wed |
| 3. J/Psi production as a function of event activity in p+p collisions at $\sqrt{s} = 500$ GeV at STAR | | Brennan Schaefer | Wed |
| 4. Accessing the shape of cluster pattern in O+ O and d+Au collisions from STAR experiment | | Zaining Wang | Wed |
| 5. Anisotropic Flow of Identified Hadrons in O+O Collisions at $\sqrt{s_{NN}} = 200$ GeV | | Santanu Prodhan | Wed |
| 6. Study of charge and baryon transport in O+O and Au+Au collisions at $\sqrt{s_{NN}} = 200$ GeV with STAR experiment | | Wendi Lu | Wed |
| 7. Search for Exotic Particles in Multi-Prong Central Exclusive Production in pp Collisions at the STAR Experiment | | Aranya Giri | Wed |
| 8. Measurement of coherent K+K- photoproduction in Au+Au ultra-peripheral collisions at $\sqrt{s_{NN}} = 200$ with the STAR | | Luobing Wang | Wed |
| 9. $\pi/K/p/\phi$ flow in O+O and d+Au collisions | | Souvik Paul | Wed |
| 10. Engineering the shapes of quark-gluon plasma droplets by comparing anisotropic flow in small symmetric and asymmetric collision systems | | Chunjian Zhang | Wed |
| 11. The underlying event and global event-structure observables in p+p collisions at STAR | | Oliver Matonoha | Wed |